Bull. Chem. Soc. Jpn., 73, 1581—1587 (2000)


# Site-Selective X-Ray Absorption Fine Structure (XAFS) Spectroscopy (2). XAFS Spectra Tuned to Surface Active Sites of Cu/ZnO and Cr/$SiO_2$ Catalysts

**Yasuo Izumi*** **and Hiroyasu Nagamori**

Department of Environmental Chemistry and Engineering, Interdisciplinary Graduate School of Science and Engineering, Tokyo Institute of Technology, 4259 Nagatsuta, Midori-ku, Yokohama 226-8502

(Received January 20, 2000)

Site-selective XAFS spectra were measured by tuning the Rowland-type fluorescence spectrometer to each site of Cu/ZnO and Cr/$SiO_2$ catalysts. The chemical shifts between $Cu^0$ and $Cu^I$ sites and between $Cr^{III}$ and $Cr^{VI}$ sites were relatively large for model compounds ($\Delta E = 1.6$ eV), and were utilized as the tune energies of site-selective XAFS. Site-selective XANES tuned to $Cu^0$, $Cu^I$, and $Cr^{III}$ sites were successfully obtained. Based on the correlation between the chemical shift and the peak width (energy resolution of the fluorescence spectrometer), site-selective XANES spectra were analyzed. The population ratio of Cu metal, $Cu_2O$, and $Cu^I$ atomically dispersed on ZnO was estimated to be 70(±23) : 22(±14) : 8(±5). The contribution of the $Cr^{III}$ site to site-selective XANES tuned to the $Cr^{III}$ site was 94(±3)%.

XAFS has been widely used as a powerful tool for understanding local geometric and electronic structures. A problem of XAFS is to obtain average information about sites when the sample consists of more than one kind of site. As an experimental approach to solve this problem, a Rowland-type fluorescence spectrometer was designed, and the emission spectra were reported as the preparation of site-selective XAFS.[1] The chemical shift for the Cu $K\alpha$ peak was +1.6 eV on going from $Cu^0$ to $Cu^I$ (CuCl) and that for Cr $K\beta_1$ peak was −1.6 eV on going from $Cr^{III}$ ($Cr_2O_3$) to $Cr^{VI}$ ($K_2CrO_4$).

The feasibility of site-selective XAFS by utilizing a fluorescence spectrometer was reported.[2] Site-selective XAFS was applied to manganese inorganic complexes. Other site-selective XAFS approaches have been reported concerning studies of catalysts and related solid materials: photon-stimulated ion desorption study for $O^+$ on a Mo(100) surface,[3] total-reflection fluorescence study for surface Mo species,[4] a capacitance study related to a deep-level trap for Se-doped $Al_{1/3}Ga_{2/3}As$,[5] and the combination of XANES and XMCD (X-ray magnetic circular dichroism) for nickel ferrites.[6] The aim of this study is to apply site-selective XAFS spectroscopy to heterogeneous catalyst surface active sites. Cu/ZnO catalysts synthesize methanol from CO (and/or $CO_2$) + $H_2$. Practically, a third component, such as $Al_2O_3$, $Cr_2O_3$, or $La_2O_3$, is added.[7—9] However, the reaction mechanism has not been fully clarified primarily because the Cu exists in various phases, even for the binary system of Cu/ZnO. The importance of the $Cu^I$–O–Zn species for methanol synthesis has been proposed.[10] The reaction route to methanol is also controversial: a direct route to methanol vs. an indirect route from $CO_2$ produced by a water-gas shift reaction.[11,12] Cu metal, Cu microcluster, $Cu_2O$, and $Cu^I$ atomically dispersed on ZnO were reported for Cu/ZnO catalysts by means of XANES (X-ray absorption near-edge structure) and EXAFS (extended X-ray absorption fine structure).[13] As the Cu content in the catalyst increased from 1 to 10%, the relative population of the $Cu^0$ and $Cu^I$ sites changed from 37 to 45% and from 63 to 55%, respectively. The methodology of this study was to *experimentally* measure the XAFS spectra of $Cu^0$ sites (Cu metal phase) and $Cu^I$ sites ($Cu_2O$ and $Cu^I$ atomically dispersed on ZnO) separately.

The $Cu^0$ and $Cu^I$ sites may be both inevitable components for methanol synthesis in bifunctional or synergetic reaction mechanism for hydrogen activation, intermediate (formate, formyl, etc.) formation, and transformation to product.[14,15] The active site of Cr/$SiO_2$ catalysts is reduced in an oxidative cycle and is oxidized in a reductive cycle in the partial oxidation of alcohols.[16,17] Inactive $\alpha$-chromia-like cluster species coexist in catalysts.[16,18] It is important to obtain both geometric and electronic structure information about the active site in the oxidized form, $Cr^{VI}$, and in the reduced form, $Cr^{III}$ (or $Cr^{II}$) separately.

This paper deals with the site-selective XANES spectra for Cu/ZnO and Cr/$SiO_2$ catalysts to obtain each site electronic state and the relative population of sites. The obtained data are compared to the chemistry obtained by conventional XAFS.[13,18]

## Experimental

**Sample Preparation.** Standard samples of $CuCl_2$, $Cu_2O$, CuO, $Cr_2O_3$, and $K_2CrO_4$ were prepared in a similar method to that described in Ref. 1. A Cu/ZnO catalyst was prepared by the co-precipitation method.[8,11,14] Copper and zinc nitrates (Wako) were dissolved in water, and co-precipitated by adding a sodium carbon-

ate solution. The solution was stirred for 1 h, followed by filtration and washing with water. The obtained powder was dried at 393 K for 15 h, and calcined at 623 K for 4 h. The Cu content was 5 wt%. The sample was introduced into a glass *U*-tube connected to a closed circulation system, and heated in $H_2$ (53 kPa) at 523 K for 1 h and in CO (27 kPa) and $H_2$ (27 kPa) at 523 K for 1 h. The thus-activated catalyst was transferred to an in-situ Pyrex® glass cell equipped with 50 μm-thick Kapton windows on both sides. The cell was sealed by fire, and transported to SPring8. The activity of the catalyst was tested after the beamtime. The activity measured during XAFS sample preparation was reproduced. Hence, the electronic and geometric information obtained by XAFS in this work is closely related to the in-situ active site.

A $Cr/SiO_2$ catalyst was prepared by the incipient wetness method.[16,18] A $CrO_3$ solution was reacted with $SiO_2$ (Davison 952) at 293 K for 0.5 h. The water was evaporated, and the obtained powder was dried at 373 K for 6 h. The Cr content was 15 wt%. The sample was evacuated at 293 K for 0.5 h, and interacted with ethanol (10 kPa) at 373 K for 5 h. The color changed from orange to green. The thus-prepared catalyst was pressed into a disk ($\phi$ = 10 mm, 30 mg).

**Emission and XANES Spectrum Measurements.** The Cu $K\alpha$ emission spectra and the Cu K-edge site-selective XANES spectra were measured at the Undulator beamline 10XU of SPring8 (Proposal No. 1999B0220-NX-np, 1998A0295-NX-np). The design of a fluorescence spectrometer equipped with a Ge(111) crystal was described in Ref. 1. The storage-ring energy was 8.0 GeV and the ring current was 99—74 mA. A Si(111) double-crystal monochromator was used. Special or different points from Ref. 1 are briefly described. The catalyst sample sealed in an in-situ glass cell was set on the sample holder. The height of the sample holder was controlled by a micrometer so that the incident X-ray beam made a spot at the center of the sample surface. Because the sample was sealed in 53 kPa of $CO+H_2$, the Kapton film window was slightly curved inside due to the pressure difference. The angles $\theta$ and $\chi$ were optimized for the fluorescence X-ray intensity at SC (scintillation counter, Fig. 1 of previous paper).[1] As a result, both angles were set to be 13° during spectrum scan.

All of the Cu emission and XANES spectra were obtained with the sample completely covered with 1 mm-thick lead plates, except for the primary beam entrance and the fluorescence X-ray beam exit toward the bent crystal. The excitation energy was 9000.1 eV. Ge(444) reflection was utilized in the fluorescence spectrometer. The parameters of a wide scan of the $K\alpha_1$ and $K\alpha_2$ region were a 0.01° step of the Bragg angle (ca. 0.5 eV), 60 s accumulation for a step, and 80 steps for a spectrum. Those of a narrow scan of the $K\alpha_1$ region were 0.0025° step (ca. 0.12 eV), 60 s accumulation for a step, and 100 steps for a spectrum. The peak positions were reproduced within 0.2 eV when several emission spectra were scanned. The Cu emission energy was calibrated by equalizing the Cu foil $K\alpha_1$ peak top to 8047.8 eV.[19]

Site-selective Cu K-edge XANES spectra were measured by tuning the fluorescence spectrometer at 8048.8 eV ($\theta_B$ = 70.610°) for $CuCl_2$ and at 8046.6 eV (70.654°) and 8050.9 eV (70.567°) for Cu/ZnO catalyst based on the peak energies of the emission spectra. The accumulation time of a step was 10—15 s. The spectra were calibrated by equalizing the first inflection point of the Cu foil K-edge to 8980.3 eV.[19]

The Cr $K\beta$ emission spectra and Cr K-edge site-selective XANES spectra were measured at bending-magnet beamline 7C of KEK-PF (Proposal No. 99G060). The ring operation conditions are given in Ref. 1. The excitation energy was 6020.9 eV. Ge(333) reflection was utilized in the fluorescence spectrometer. The peak positions were reproduced within 0.2 eV. Cr emission spectra were calibrated by equalizing the Cr foil $K\beta_1$ peak top to 5946.7 eV.[19]

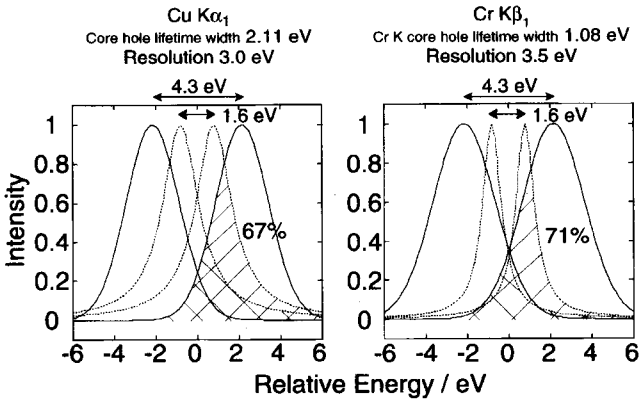


Fig. 1. The estimation of site selection for Cu $K\alpha_1$ (left) and Cr $K\beta_1$ (right). Two emission peaks (Gaussian) separated by 4.3 eV and two peaks of core hole lifetime width (Lorentzian) separated by 1.6 eV are drawn.

Site-selective Cr K-edge XANES spectra were measured by tuning the fluorescence spectrometer at 5947.5 eV ($\theta_B$ = 73.218°) for the $Cr/SiO_2$ catalyst based on the emission spectra. The accumulation time of a step was 60 s. The spectra were calibrated by equalizing the first inflection point of the Cr foil K-edge to 5988.8 eV.[19]

A smooth background was subtracted by fitting a polynomial to the pre-edge region and subtracting the polynomial from the entire XANES spectrum. Normalization of the Cu and Cr K-edge data was accomplished by fitting a flat polynomial to the post-edge region and normalizing the edge jump to 1.0 at 9040 and 6050 eV, respectively.[20] The normalization at the energies was verified by normalizing the XANES spectra over wider region (150—200 eV). The normalization procedure can produce a maximum of a 3% difference in the pre-edge peak intensity.

## Results

The FWHM (full width at a half maximum) of the emission peaks was found to be controlled by the geometrical angle width (slit size). The FWHM of Cu $K\alpha_1$ and $K\alpha_2$ was as small as 3.0 eV.[1] Figure 1 illustrates two emission peaks (Gaussian) separated by 4.3 eV and two peaks of the core hole lifetime width (Lorentzian) separated by 1.6 eV, assuming the 1 : 1 intensity ratio of two peaks. In the case of a FWHM of 3.0 eV for Cu $K\alpha_1$, the ratio of the overlap area (hatched in Fig. 1) with a Gaussian for the two Lorentzians was 67 : 33. The FWHM of Cr $K\beta_1$ was as small as 3.7 eV.[1] This case is similar to Fig. 1, right. The ratio of the overlap area with a Gaussian for the two Lorentzians was 71 : 29.

**Cu $K\alpha$ Emission Spectra for Cu/ZnO.** Cu $K\alpha$ emission spectra were measured for the Cu/ZnO catalyst activated in CO + $H_2$ at 523 K. The obtained spectrum is depicted in Fig. 2a. The peak energies and FWHM obtained by a Gaussian fit are listed in Table 1a. The energy splitting of the $K\alpha_1$ and $K\alpha_2$ peaks was 19.9 eV, similar to a reference value (19.8 eV).[21] The $K\alpha_1$ and $K\alpha_2$ peak positions shifted by +0.9 and +0.6 eV, respectively, compared to the corresponding peaks for a Cu foil (8047.8 and 8028.2 eV).[1] These shifts

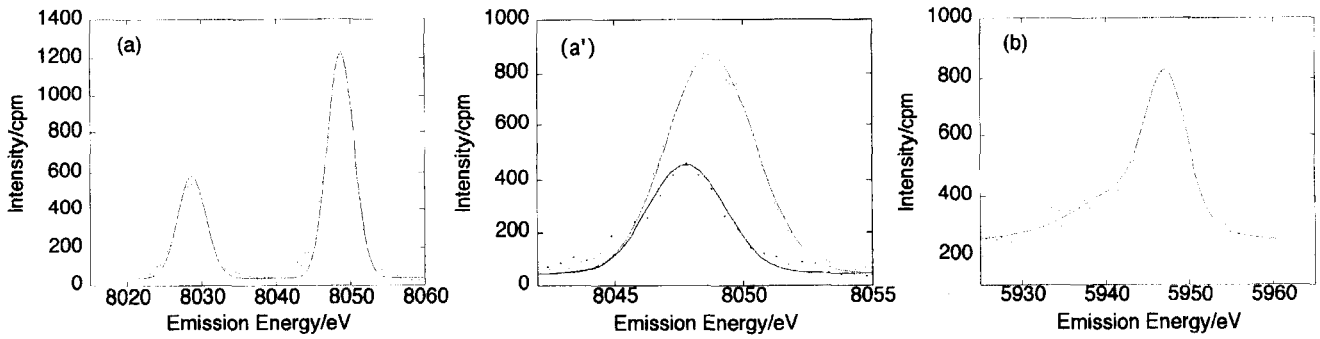


Fig. 2. Cu $K\alpha$ emission spectra of Cu/ZnO catalyst (a) and Cr $K\beta$ emission spectra of $Cr/SiO_2$ catalyst (b). The experimental data are plotted as points and the Gaussian fittings are drawn as solid curves. These spectra correspond to Table 1. The Cu $K\alpha_1$ region was measured with smaller scan step (ca. 0.12 eV) for Cu/ZnO (top of a'), and compared to Cu foil spectra (bottom of a').

Table 1. Peak Energies and FWHM of Cu $K\alpha_1$ and $K\alpha_2$ in the Emission Spectra of Cu/ZnO (a) and Cr $K\beta_1$ and $K\beta'$ in the Emission Spectra of $Cr/SiO_2$ (b)

(a) Cu $K\alpha$ emission

| Sample | Peak energy/eV | | | FWHM/eV | |
|---|---|---|---|---|---|
| | $K\alpha_1$ | $K\alpha_2$ | Split | $K\alpha_1$ | $K\alpha_2$ |
| Cu/ZnO | 8048.7 | 8028.8 | 19.9 | 4.0 | 4.0 |

(b) Cr $K\beta$ emission

| Sample | Peak energy/eV | | | FWHM/eV | |
|---|---|---|---|---|---|
| | $K\beta_1$ | $K\beta'$ | Split | $K\beta_1$ | $K\beta'$ |
| $Cr/SiO_2$ | 5947.3 | 5939.8 | 7.5 | 6.7 | 6.7 |

The size of slit 0 was $1.0\times1.0$ mm$^2$ for (a) and $2.0\times1.0$ mm$^2$ for (b). The size of slits 1 and 2 was $8.0\times1.0$ mm$^2$ for (a) and $8.0\times5.5$ mm$^2$ for (b).

were larger than the reproducibility of the energy position of this spectrometer at Cu $K\alpha$ (< 0.2 eV). The energy positions of Cu/ZnO were near $Cu^{II}$ (8048.8 and 8029.2 eV for $CuCl_2$).[1]

The $K\alpha_1$ peak region was scanned more carefully with ca. 0.12 eV steps (Fig. 2a', top). The FWHM was larger for Cu/ZnO (4.0 eV) than those for Cu foil (3.5 eV, Fig. 2a', bottom) with the same size of three slits (slit 0 in front of $I_0$ ion chamber, slit 1 between sample and bent crystal, and slit 2 in front of SC, see Fig. 1 of Ref. 1 and footnotes of Table 1). A possible reason for the difference is that the former spectrum consists of (more than) two peaks. Two Gaussian peaks of FWHM 3.5 eV separated by 1.6 eV form a convoluted peak of FWHM 4.086 eV, similar to the FWHM of 4.0 eV for Cu/ZnO. The chemical shift on going from $Cu^0$ to $Cu^I$ may be ca. +1.6 eV for Cu/ZnO. This estimation is consistent with the chemical shift on going from Cu to CuCl (+1.6 eV).[1]

**Cr $K\beta$ Emission Spectrum for $Cr/SiO_2$.** Cr $K\beta$ emission spectra were measured for the $Cr/SiO_2$ catalyst reacted with ethanol at 373 K. The obtained spectrum is depicted in Fig. 2b. The peak energies and FWHM obtained by a Gaussian fit to the main peak and a shoulder peak (two functions) are listed in Table 1b. The $K\beta_1$ and $K\beta'$ peak energies were similar to those of $Cr_2O_3$ (5947.5 and 5939.9 eV).[1] The differences (0.1—0.2 eV) were on an equivalent level of reproducibility of the peak energy (< 0.2 eV) at the energy of Cr $K\beta$. The FWHM of $K\beta_1$ for $Cr/SiO_2$ (6.7 eV) was larger than those for $Cr_2O_3$ and $K_2CrO_4$ (5.3—6.2 eV), suggesting the presence of a minor $Cr^{VI}$ site in addition to the major $Cr^{III}$ site.

**Site-Selective XANES for Cu.** The Cu K-edge XANES spectrum was measured for $CuCl_2$ by tuning the fluorescence spectrometer at 8048.8 eV (peak top of Cu $K\alpha_1$ for $CuCl_2$). The obtained XANES spectrum is drawn in Fig. 3. The edge and pre-edge peak positions and the pre-edge peak area are listed in Table 2. The shoulder peak at 8990 eV was better resolved than in the case of conventional fluorescence XANES[22] (Fig. 3 inset, dotted line). The pre-edge peak at 8980.4 eV was clearly observed in XANES obtained by using a fluorescence spectrometer, compared to a more flat and obscure feature in the conventional fluorescence XANES. The $I$ signal in the case utilizing a fluorescence spectrometer is counted if the fluorescence X-ray satisfies the Rowland configuration compared to conventional XANES where the $I$ signal counts all the fluorescence X-ray from sample. Similar effects to the slit size in front of the $I_0$ chamber vs. XANES energy resolution are implied for the higher energy resolution

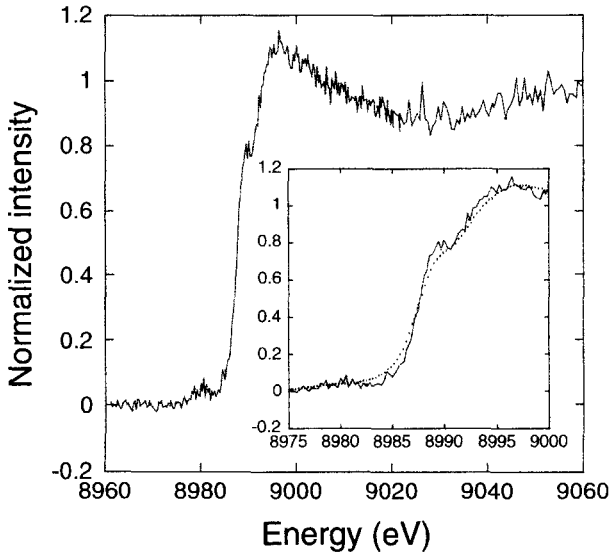


Fig. 3. Site-selective XANES spectrum for $CuCl_2$ tuned to 8048.8 eV (solid line), and corresponding conventional XANES measured by Lytle detector (inset, dotted line).

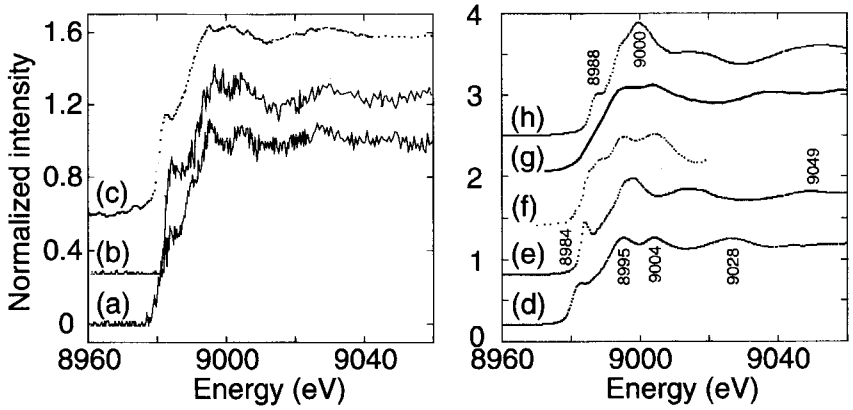


Fig. 4. Site-selective XANES spectra for Cu/ZnO catalyst. Fluorescence spectrometer was tuned to 8046.6 eV (a) and to 8050.9 eV (b). Conventional XANES spectra for Cu/ZnO (c), Cu foil (d), $Cu_2O$ (e), [Cu(tepa)][$BPh_4$] (f), and CuO (h) were measured by Lytle detector (c) or in transmission mode (d, e, h). XANES was theoretically generated by FEFF8 for $Cu^I$ atomically dispersed on ZnO (g). XANES of [Cu(tepa)][$BPh_4$] was reproduced from Ref. 13.

Table 2. The Edge and Pre-edge Peak Positions and Pre-edge Peak Areas of Site-Selective XANES Spectra for Cu/ZnO Catalyst Tuned to $Cu^0$ and $Cu^I$ Sites, for $CuCl_2$ Tuned to $Cu^{II}$ Site, and for $Cr/SiO_2$ Catalyst Tuned to $Cr^{III}$ Site

| Sample | Site | K-edge | Pre-edge peak | |
|---|---|---|---|---|
| | | position/eV | Position/eV | Area/eV |
| Cu/ZnO | $Cu^0$ | 8981.3 | — | — |
| | $Cu^I$ | 8982.4 | — | — |
| $CuCl_2$ | $Cu^{II}$ | 8987.8 | 8980.4 | 0.19 |
| $Cr/SiO_2$ | $Cr^{III}$ | 6002.4 | 5992.9 | 0.11 |

in the case utilizing a fluorescence spectrometer.

The conventional fluorescence XANES spectrum for the Cu/ZnO catalyst (Fig. 4c) did not have a shoulder at 8988 eV nor a peak top at 9000 eV, which were typical for CuO XANES (Fig. 4h). The possibility that the $Cu^{II}$ site co-exists in the Cu/ZnO catalyst was neglected, and the targets of site-selective XANES were the $Cu^0$ and $Cu^I$ sites. The three-slit size of the fluorescence spectrometer was the same as that for the Cu emission spectrum. The fluorescence energies corresponding to the half maximum of the observed peak (Fig. 2a′, top) were chosen as each tune energy.

The Cu K-edge XANES spectra for Cu/ZnO by tuning the fluorescence spectrometer at 8046.6 and 8050.9 eV are shown in Figs. 4a and 4b, respectively. The pattern of Fig. 4a resembles that of Fig. 4d (Cu foil). The peak top positions at 8995, 9004, and 9028 eV were common for the two spectra. The broad peak at 9049 eV of Fig. 4a also appeared in Fig. 4e ($Cu_2O$). The first shoulder peak at 8982—8984 eV consisted of a complex curve, which may have been generated with the sum of Figs. 4d and 4e.

The rising edge position shifted to higher energy for Fig. 4b compared to Fig. 4a, demonstrating the contribution from the $Cu^I$ site. The peak top position at 8984 eV was the same as that of Fig. 4e ($Cu_2O$), and assigned as the $1s \rightarrow 4p$ electronic dipole transition.[23] The region of 8993—9008 eV was intense, similar to the case of Fig. 4e, though the peak split into two peaks. The peak top position at 9028 eV was the same as that of Fig. 4d (Cu foil).

**Site-Selective XANES for Cr.** The Cr K-edge XANES spectrum was measured for the $Cr/SiO_2$ catalyst by tuning the fluorescence spectrometer at 5947.5 eV. The energy corresponds to the $K\beta_1$ peak top for $Cr_2O_3$.[1] The obtained XANES spectrum is shown in Fig. 5a. The XANES pattern was similar to that of $Cr_2O_3$ XANES (Fig. 5c). The spectrum was different from conventional fluorescence XANES for the $Cr/SiO_2$ catalyst (Fig. 5b). The pre-edge peak area was 0.11 and 0.39 eV for Figs. 5a and 5b, respectively (Table 2). An intense pre-edge peak was observed for $K_2CrO_4$ (Fig. 5d).

## Analysis

The conventional fluorescence XANES spectrum for Cu/ZnO (Fig. 4c) was simulated by the convolution of two

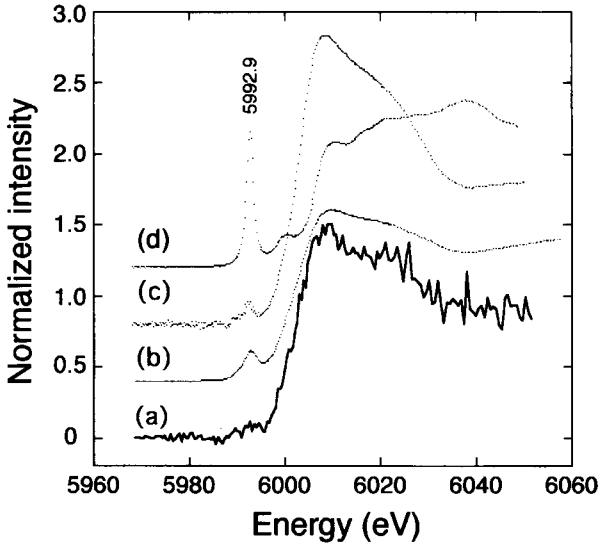


Fig. 5. Site-selective XANES spectra for $Cr/SiO_2$ catalyst. Fluorescence spectrometer was tuned to 5947.5 eV (a). Conventional XANES spectra for $Cr/SiO_2$ (b), $Cr_2O_3$ (c), and $K_2CrO_4$ (d) measured by Lytle detector (b) or in transmission mode (c, d).

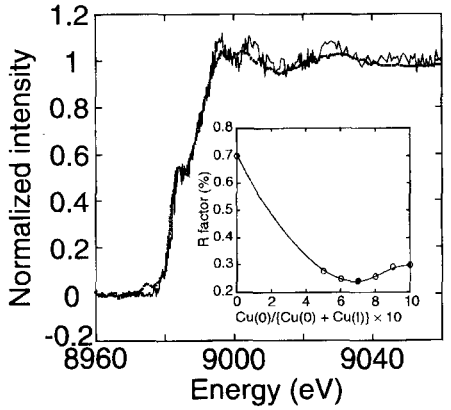


Fig. 6. Conventional XANES of Cu/ZnO catalyst (dotted line) and the best fit by the convolution of site-selective XANES tuned to 8046.6 and 8050.9 eV (solid line). The best-fit intensity ratio of two site-selective XANES was 7 : 3 (inset).

site-selective XANES spectra tuned to $Cu^0$ and $Cu^I$ sites (Figs. 4a and 4b). The ratio was varied between 10 : 0 and 0 : 10. The generated convoluted spectrum most resembled the conventional Cu/ZnO XANES when the ratio was 7 : 3 (Fig. 6). The fit was evaluated based on the $R$ factor $(R_f) = \int|\chi(\text{exp}) - \chi(\text{fit})|^2 dE / \int|\chi(\text{exp})|^2\, dE$ (Fig. 6, inset).

The site-selective XANES spectrum tuned to the $Cu^0$ site (Fig. 4a) was simulated by the convolution of Cu metal and $Cu_2O$ XANES. The $R_f$ value was minimum when the intensity ratio was 8 : 2 (dotted line in Fig. 7a). The site-selective XANES spectrum tuned to the $Cu^I$ site (Fig. 4b) was simulated by convoluting the theoretically-generated XANES for the $Cu^I$ site atomically dispersed on ZnO(0001) (calculated by FEFF8[24,25] for a model cluster within 6 Å from the absorbing Cu atom on the wurzite ZnO(0001) surface in a self-consistent field and multiple scattering modes) and $Cu_2O$ XANES (Figs. 4g and 4e, respectively). Because the theoretical XANES for the $Cu^I$ site on ZnO is similar to XANES for the model complex [Cu(tepa)][$BPh_4$] (tepa = $N(CH_2CH_2$-2-pyridyl)$_3$)[26] in Fig. 4f, the theoretical XANES was used for the fit. The $R_f$ value was minimum when the intensity ratio was 5 : 5. However, the fit was not satisfactory ($R_f$ 0.63%) compared to the above-mentioned two fits ($R_f$ 0.23 and 0.31%). A simulation by the convolution of Cu metal and $Cu_2O$ was not satisfactory either ($R_f$ 0.64%). Thus, the simulation was performed by adding conventional XANES of Cu metal (Fig. 4d) to the 5 : 5 convolution of theoretical XANES for the $Cu^I$ site on ZnO and $Cu_2O$ XANES, by changing the $Cu^0$ : $Cu^I$ ratio from 10 : 0 to 0 : 10. The best fit is drawn as a dotted line in Fig. 7b for a ratio of 5 : 5 (inset).

## Discussion

**Basic Parameters for Site-Selective XAFS.** Site-selective XANES spectra were obtained for the $Cu^{II}$ site for the $CuCl_2$, $Cu^0$ and $Cu^I$ sites for the Cu/ZnO catalyst, and the $Cr^{III}$ site for the $Cr/SiO_2$ catalyst. Although copper dichloride consists of only a $Cu^{II}$ site, the obtained spectrum by tuning the fluorescence spectrometer to 8048.8 eV was not identical to the conventional fluorescence XANES (Fig. 3). By using a fluorescence spectrometer, the energy resolution of the XANES spectrum was improved over that of the conventional fluorescence XANES, as demonstrated by the sharpness of the pre-edge and shoulder peaks.

A correlation between the emission peak width and the chemical shift (Fig. 1) determines how effectively the site-selective XANES spectra are obtained. The chemical shift on going from Cu metal ($Cu^0$) to CuCl ($Cu^I$) was +1.6 eV, and that on going from $Cr_2O_3$ ($Cr^{III}$) to $K_2CrO_4$ ($Cr^{VI}$) was −1.6 eV.[1] The parameters of the fluorescence spectrometer (three slits size) were common for the emission spectrum (Table 1 and Fig. 2) and site-selective XANES measurements (Figs. 4 and 5). The FWHM of the main emission peaks for Cu/ZnO and $Cr/SiO_2$ catalysts were 4.0 and 6.7 eV (Table 1), respectively, larger than those for a Cu foil (3.5 eV) and $Cr_2O_3$ and $K_2CrO_4$ (5.3—6.2 eV), respectively.[1] Therefore, the emission spectra for the Cu/ZnO and $Cr/SiO_2$ catalysts were suggested to consist of (more than) two peaks

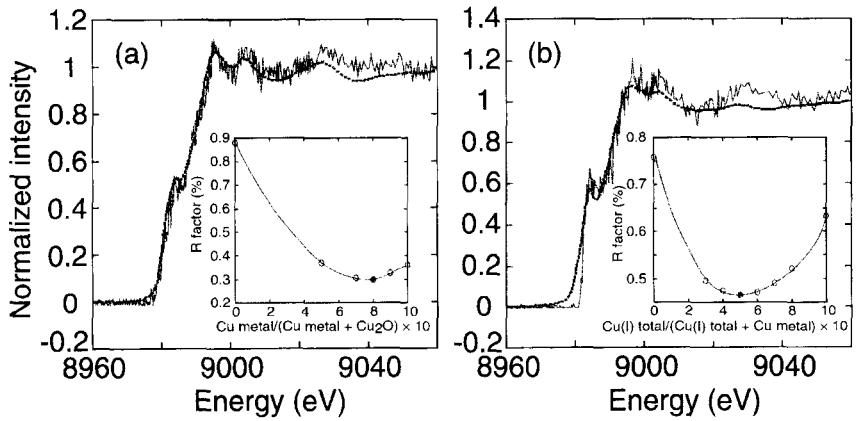


Fig. 7. (a) Site-selective XANES of Cu/ZnO catalyst tuned to 8046.6 eV (solid line) and the best fit by the convolution of Cu metal and $Cu_2O$ XANES (dotted line). The best-fit intensity ratio was 8 : 2 (inset). (b) Site-selective XANES of Cu/ZnO catalyst tuned to 8050.9 eV (solid line) and the best fit by the convolution of Cu metal, $Cu_2O$, and $Cu^I$ / ZnO XANES (dotted line). The intensity ratio of $Cu_2O$ and $Cu^I$ / ZnO XANES was first optimized to be 5 : 5, then the intensity ratio of Cu metal and $Cu^I$ total ( = $Cu_2O$ 5 + $Cu^I$/ZnO 5) was optimized to be 5 : 5 (inset).

Table 3. The Population Ratio of Copper States in Cu/ZnO Catalysts (Cu 5 wt%) Estimated by Site-Selective XANES and in Reference

| Condition | Population/% | | | |
|---|---|---|---|---|
| | Cu metal | $Cu_2O$ | $Cu^I$ atomically dispersed on ZnO | Reference |
| in CO + $H_2$, 523 K | 70(±23) | 22(±14) | 8(±5) | This work |
| in $H_2$, 523 K | 80(±10) | 20(±10) | — | This work |
| in CO + $CO_2$ + $H_2$, 493 K | 37 | 26 | 37 | 13 |

originating from different sites.

Two 3.5 eV-width peaks originating from the $Cu^0$ and $Cu^I$ sites were assumed in the emission spectra of Cu/ZnO (Fig. 2a′), separated by ca. 1.6 eV. A rough estimation of the $Cu^0$ or $Cu^I$-site selectivity is 67% when the tune energies are separated by 4.3 eV (Fig. 1). The three-slit size of the fluorescence spectrometer determines the peak width rather than the Rowland radius and X-ray penetration depth into a bent crystal.[1] Better selectivity up to 69% was expected by decreasing the FWHM 2.0 eV.

**Interpretations of Site-Selective XANES Spectra.** Site-selective XANES spectra were measured by tuning the fluorescence spectrometer at 8046.6 and 8050.9 eV for the Cu/ZnO catalyst (Figs. 4a and 4b). Based on their edge shift and peak pattern, they are basically attributed to the $Cu^0$ and $Cu^I$ sites, respectively. The convoluted peak of site-selective XANES tuned to the $Cu^0$ and $Cu^I$ sites (Figs. 4a and 4b) most resembled the conventional fluorescence Cu/ZnO XANES (Fig. 4c) when the ratio was 70 : 30 (Fig. 6). The site-selective XANES spectrum tuned to the $Cu^0$ site (8046.6 eV) was best fitted by the convolution of Cu metal 80+$Cu_2O$ XANES 20. The site-selective XANES spectrum tuned to the $Cu^I$ site (8050.9 eV) was simulated by the convolution of Cu metal 50+$Cu_2O$ 25+$Cu^I$/ZnO XANES 25. The relatively poorer fits in Fig. 7b may be an inappropriate model (theoretically generated XANES or [Cu(tepa)][$BPh_4$]) of $Cu^I$ site atomically dispersed on ZnO. The $Cu^I$ site of [Cu(tepa)][$BPh_4$] has a distorted $C_{3v}$ symmetry (Cu–$N_{ammine}$ 2.192, Cu–$N_{pyridyl}$ 2.012—2.022 Å, $N_{ammine}$–Cu–$N_{pyridyl}$ 97.4—99.2°).[26] The coordination of the $Cu^I$ site on ZnO(0001) in $C_{3v}$ symmetry was proposed by means of variable-energy photoelectron spectroscopy.[27]

Based on three XANES fits (Figs. 6 and 7), the population ratio of Cu metal, $Cu_2O$, and $Cu^I$ atomically dispersed on ZnO is estimated to be 70(±23) : 22(±14) : 8(±5) (Table 3). Table 3 also lists the reported population ratio for Cu 5 wt% Cu/ZnO catalyst.[13] Conventional XANES for Cu/ZnO before a CO+$H_2$ treatment (i.e., in $H_2$ at 523 K) was fitted with Cu metal XANES 80+$Cu_2O$ XANES 20 (Table 3, fit is not shown). Hence, a part of the Cu metal site (8—10%) is suggested to disperse on ZnO as an atomic $Cu^I$ site during the CO/$H_2$ reaction due to the effect of CO gas. The increase of the $Cu^I$ site atomically dispersed on ZnO corresponded to the methanol synthesis rate. Because the $Cu^I$ site atomically dispersed on ZnO did not increase due to the extended reaction in CO+$H_2$ at 523 K than 1 h, the difference between our data and Ref. 13 for Cu/ZnO during catalysis may be due to the difference in the pretreatment temperature. Our sample was calcined at 623 K compared to 573 K for Ref. 13. A pretreatment under a severe condition may preferably produce metallic Cu. Another possibility is that the reaction gas was CO+$H_2$ (523 K) in this study, compared to CO+$CO_2$+$H_2$ (493 K) in Ref. 13. Carbon dioxide may disperse part of the metallic copper on ZnO as $Cu^I$ more effectively by an oxidative effect. The color of the Cu/ZnO catalyst dramatically changed from black to red-brown during activation in CO+$H_2$ at 523 K.

In the case that the site population ratio of Cu metal, $Cu_2O$, and $Cu^I$ atomically dispersed on ZnO is 70 : 22 : 8, site-selective XANES tuned to the $Cu^0$ site obtained a major signal from Cu metal, but the XANES tuned to the $Cu^I$ site was affected by severe tailing of the Cu metal emission peak. In fact, the site-selective XANES in Fig. 4a was quite similar to Cu foil XANES, but the site-selective XANES in Fig. 4b was not similar to $Cu_2O$ nor [Cu(tepa)][$BPh_4$] XANES.

Site-selective XANES was also tried for the Cr K-edge (Fig. 5). Chromium was chosen due to a relatively larger chemical shift and a smaller natural core-hole lifetime of the K level (1.08 eV) compared to the case of Cu (1.55 eV) (Fig. 1).[28] The disadvantage of Cr site-selective XANES was a weaker fluorescence X-ray intensity (at ca. 5950 eV); even the acrylic house of fluorescence spectrometer was purged in helium.[29] The site-selective XANES spectrum tuned to 5947.5 eV of the Cr/$SiO_2$ catalyst (Fig. 5a) had a weaker pre-edge peak than that of the conventional fluorescence XANES, which is ascribed to the $1s \rightarrow 3d$ electronic transition, typical for the $Cr^{VI}$ site.[18,30] The post-edge pattern became similar to $Cr_2O_3$ XANES (Fig. 5c). Thus, the possibility of site-selective XAFS was also demonstrated for the $Cr^{III}$ site. Based on the pre-edge peak area (Table 2, the area was 1.81 eV for $K_2CrO_4$), site-selective XANES tuned to 5947.5 eV consisted of a contribution of 94(±3)% from the $Cr^{III}$ site, whereas the conventional XANES consisted of 78(±2)% of the $Cr^{III}$ site contribution. The monitored $Cr^{III}$ site was either reduced from $Cr^{VI}$ by a reaction with ethanol or inert crystalline of $\alpha$-$Cr_2O_3$.[16—18] Site-selective XANES tuned to $Cr^{VI}$ site was unsuccessful for the Cr/$SiO_2$ catalyst. The larger population of the $Cr^{III}$ site than the $Cr^{VI}$ site was the major reason. The $Cr^{VI}$ $K\beta_1$ peak shifted to a lower energy than $Cr^{III}$ $K\beta_1$, and $Cr^{III}$ $K\beta'$ exists near $Cr^{VI}$ $K\beta_1$. The overlap of the $K\beta'$ peak is another reason for the difficulty to tune to the $Cr^{VI}$ site.

## Summary

Site-selective XAFS was applied to Cu/ZnO and Cr/$SiO_2$ catalysts. In the emission spectra, the FWHM of Cu/ZnO and

$Cr/SiO_2$ catalysts was 4.0 and 6.7 eV (Table 1), respectively, greater than the values for Cu foil (3.5 eV) and for $Cr_2O_3$ and $K_2CrO_4$ (5.3—6.2 eV).[1] The emission spectra for catalysts should consist of (more than) two sites. The chemical shift of two component peaks was suggested to be ca. 1.6 eV for Cu/ZnO. The fluorescence spectrometer was tuned to an energy corresponding to the half maximum of the emission peak.

The site-selective XANES spectra for the Cu/ZnO catalyst tuned to the $Cu^0$ and $Cu^I$ sites (Fig. 4) were analyzed (Figs. 6 and 7) based on the standard XANES spectra for the Cu foil, $Cu_2O$, theoretical XANES generated by FEFF8 for $Cu^I$ site atomically dispersed on ZnO, and CuO. The population ratio of Cu metal, $Cu_2O$, and $Cu^I$ atomically dispersed on ZnO was estimated to be $70(\pm23):22(\pm14):8(\pm5)$. It was important to experimentally measure the $Cu^0$ and $Cu^I$ sites XANES separately to facilitate the XANES analysis. However, the analysis had a minor problem to fit the site-selective XANES spectra tuned to the $Cu^I$ site, probably due to an inappropriate model of the $Cu^I$ site atomically dispersed on ZnO. Site-selective XANES was also successfully obtained for the $Cr^{III}$ site of the $Cr/SiO_2$ catalyst (Fig. 5).

In order to obtain site-selective XAFS routinely, a smaller primary beam size (less than 100 μm) and stability of the beam position should be necessary. Site-selective XANES was measured at the Undulator beamline SPring8 10XU, the brightest X-ray beamline, to obtain a better signal/noise ratio for the *I* signal. Because EXAFS needs a better signal/noise ratio than XANES, site-selective EXAFS will need an enormous scan time (longer than 10 h). In the future, a brighter X-ray source and/or a multicrystal fluorescence spectrometer[31] will enable site-selective EXAFS within a reasonable scan time.

This work was supported by grants from Toray Science Foundation (No. 98-3901, Y.I.), Kanagawa Academy of Science and Technology (Nos. 9991008 and 12740376, Y.I.), and Grants-in-Aid for Scientific Research from the Ministry of Education, Science, Sports and Culture (Monbusho) (No. 08874066, Y.I. and No. 10355032, Prof. K. Aika). We thank Dr. M. Ishii and Dr. H. Tanida (SPring8) for instructions about beamline 10XU and Prof. M. Nomura (KEK-PF) for instructions about beamline 7C.

## References

1 Y. Izumi, H. Oyanagi, and H. Nagamori, *Bull. Chem. Soc. Jpn.*, in final reviewing process.

2 M. M. Grush, G. Christou, K. Hamalainen, and S. P. Cramer, *J. Am. Chem. Soc.*, **117**, 5895 (1994).

3 R. Jaeger, J. Feldhaus, J. Haase, J. Stohr, Z. Hussain, D. Menzel, and D. Norman, *Phys. Rev. Lett.*, **45**, 1870 (1980).

4 W. Chun, K. Asakura, and Y. Iwasawa, *J. Phys. Chem. B*, **102**, 9006 (1998).

5 M. Ishii, Y. Yoshino, K. Takarabe, and O. Shimomura, *Appl. Phys. Lett.*, **74**, 2672 (1999).

6 F. Saito, T. Toyoda, T. Mori, M. Tanaka, K. Hirano, and S. Sasaki, *Physica B*, **270**, 35 (1999).

7 K. Klier, *Adv. Catal.*, **31**, 243 (1982).

8 B. S. Clausen, B. Lengeler, and B. S. Rasmussen, *J. Phys. Chem.*, **89**, 2319 (1985).

9 H. Chen, D. Liao, L. Yu, Y. Lin, J. Yi, H. Zhang, and K. Tsai, *Appl. Surf. Sci.*, **147**, 85 (1999).

10 Y. Kanai, T. Watanabe, T. Fujitani, T. Uchijima, and J. Nakamura, *Catal. Lett.*, **38**, 157 (1996).

11 S. Fujita, M. Usui, H. Ito, and N. Takezawa, *J. Catal.*, **157**, 403 (1995).

12 P. M. Jones, J. A. May, J. B. Reitz, and E. I. Solomon, *J. Am. Chem. Soc.*, **120**, 1506 (1998).

13 L. Kau, K. O. Hodgson, and E. I. Solomon, *J. Am. Chem. Soc.*, **111**, 7103 (1989).

14 R. Brush, S. E. Golunski, and M. S. Spencer, *J. Chem. Soc., Faraday Trans.*, **86**, 2683 (1990).

15 G. J. Millar, C. H. Rochester, and K. C. Waugh, *J. Chem. Soc., Faraday Trans.*, **88**, 1033 (1992).

16 W. Hill and G. Ohlmann, *J. Catal.*, **123**, 147 (1990).

17 B. Parlitz, W. Hanke, R. Fricke, M. Richter, U. Roost, and G. Ohlmann, *J. Catal.*, **94**, 24 (1985).

18 B. M. Weckhuysen, R. A. Schoonheydt, J. Jehng, I. E. Wachs, S. J. Cho, R. Ryoo, S. Kijlstra, and E. Poels, *J. Chem. Soc., Faraday Trans.*, **91**, 3245 (1995).

19 J. A. Bearden, *Rev. Mod. Phys.*, **39**, 78 (1967).

20 Y. Izumi, T. Glaser, K. Rose, J. McMaster, P. Basu, J. H. Enemark, B. Hedman, K. O. Hodgson, and E. I. Solomon, *J. Am. Chem. Soc.*, **121**, 10035 (1999).

21 M. Deutsch, G. Holzer, J. Hartwig, J. Wolf, M. Fritsch, and E. Forster, *Phys. Rev. A*, **51**, 283 (1995).

22 F. W. Lytle, R. B. Greegor, D. R. Sandstrom, E. C. Marques, J. Wong, C. L. Spiro, G. P. Huffman, and F. E. Huggins, *Nucl. Instrum. Meth. Phys. Res.*, **226**, 542 (1984).

23 L. Kau, D. J. Spira-Solomon, J. E. Penner-Hahn, K. O. Hodgson, and E. I. Solomon, *J. Am. Chem. Soc.*, **109**, 6433 (1987).

24 A. L. Ankudinov, B. Ravel, J. J. Rehr, and S. D. Conradson, *Phys. Rev. B*, **58**, 7565 (1998).

25 J. J. Rehr, J. Mustre de Leon, S. I. Zabinsky, and R. C. Albers, *J. Am. Chem. Soc.*, **113**, 5135 (1991).

26 K. D. Karlin, J. C. Hayes, J. P. Hutchinson, J. R. Hyde, and J. Zubieta, *Inorg. Chim. Acta*, **64**, L219 (1982).

27 E. I. Solomon, P. M. Jones, and J. A. May, *Chem. Rev.*, **93**, 2623 (1993).

28 M. O. Krause and J. H. Oliver, *J. Phys. Chem. Ref. Data*, **8**, 329 (1979).

29 R. Tertian and F. Claisse, "Principles of Quantitative X-Ray Fluorescence Analysis," Heyden, London (1982).

30 L. A. Grunes, *Phys. Rev. B*, **27**, 2111 (1983).

31 U. Bergmann, M. M. Grush, C. R. Horne, P. DeMarois, J. E. Penner-Hahn, C. F. Yocum, D. W. Wright, C. E. Dube, W. H. Armstrong, G. Christou, H. J. Eppley, and S. P. Cramer, *J. Phys. Chem. B*, **102**, 8350 (1998).